A Review of AVHRR-based Active Fire Detection Algorithms: Principles, Limitations, and Recommendations

Z. Li[1], Y. J. Kaufman[2], C. Ichoku[2], R. Fraser[1], A. Trishchenko[1], L. Giglio[2], J. Jin[1], X. Yu[1]

1. Canada Centre for Remote Sensing, Ottawa, Canada, K1A 0Y7
2. NASA Goddard Space Flight Center, Greenbelt, MD

September, 2000

Abstract

As an important agent of climate change and major disturbance to ecosystems, fire is drawing increased attention from both scientists and the general public alike. Remote sensing plays an important role in obtaining quick and complete information on the occurrence and development of fires. There currently exist dozens of algorithms that use different satellite sensors to detect and monitor fire activity around the world. This paper provides an overview of various AVHRR-based algorithms for detecting active burning in three general categories: single channel threshold algorithms, multi-channel threshold algorithms, and spatial contextual algorithms. Emphasis of the discussion is placed on their physical principles, merits and limitations, as well as areas of potential improvement. Recommendations are made to address some outstanding issues such as cloud cover, surface reflection, and threshold setting. Five fire detection algorithms (IGBP, MODIS, ESA, CCRS, and Giglio et al.) are compared by applying them across the Canadian boreal forest for a six-month period and comparing cumulative fire pixels with a ground-truth data set. While fire detection algorithms are generally considered to be mature relative to algorithms for mapping burned areas, the performance of the algorithms under evaluation differs drastically, some producing considerable commission and omission errors. This implies that the hot spot detection algorithms are not robust enough for global operational use and no single-sensor algorithm is optimal to generate global fire products. Suggestions are made to further explore the potential offered by both existing and future sensors that would help improve the performance of fire detection algorithms.

1. Introduction

Biomass burning has tremendous impact on the Earth's ecosystems and climate, for it drastically alters the landscape and vegetation patterns, and emits large amounts of greenhouse gases and aerosol particles (Crutzen et al. 1979, Crutzen and Andreae 1990; Kaufman et al. 1998a). Smoke aerosols may interact with cloud droplets (Kaufman and Fraser, 1997; Reid et al. 1999) and alter considerably the Earth's radiation budget (Li et al. 1995; Li, 1998). Assessment and understanding of the wide-reaching and long-lasting effects of fires on the environment and climate entails a good knowledge of the spatial distribution and temporal variation of fire activity on a global scale. This may be achieved only through the use of remote sensing technologies, which provide an efficient and economical means of acquiring fire information over large areas on a routine basis, despite various limitations and shortcomings (Justice et al. 1993; Setzer and Malingreau 1996).

Several international programs have been established towards the goal of gaining complete information on fire activity around the world using satellite sensors. These include the International Geosphere Biosphere Program, Data and Information System's (IGBP-DIS) Global Fire Product initiative (Justice and Malingreau, 1993, 1996), the World Fire Web, the ASTR World Fire Atlas (Arino and Rosaz, 1999), the MODIS Fire Product (Kaufman et al., 1998a), and many other national and regional fire programs as summarized in Gregoire et al. (2000). These activities are among those endorsed by the Global Observation of Forest Cover program (Ahern et al. 1998). The overall objective of

GOFC is to improve our understanding of the impact of forest dynamics and forest fires on the global carbon budget. Since forest fires affect both forest dynamics and the carbon budget, monitoring and mapping forest fire is a major component of GOFC.

GOFC has two requirements 1) *near-real-time detection and monitoring of fires during the fire season and 2) post-fire season mapping of the burnt areas*. These requirements respond to the needs of three fire user groups: the global change research community, policy and decision-makers, and fire managers (Ahern 2000). Specific needs for fire information are diverse among these groups. For active fire detection, the main difference in request of fire information lies in the promptness of information delivery, with fire managers and climate research community being the most and least demanding user groups, respectively. The speed of obtaining and disseminating fire information is dictated, to a large extent, by the fire monitoring systems that are reviewed in a separate paper in this book (Gregoire et al. 2000). The accuracy of fire information is a common concern for all user groups that is determined primarily by fire detection algorithms, which are the subject of this paper. The accuracy is measured in terms of levels of both commission and omission errors and the location of fires detected that should be well defined and documented.

Remote sensing of fires has been achieved using a variety of space-borne systems/sensors. The most widely used sensor for long-term and large-scale fire monitoring is the Advanced Very High Resolution Radiometer (AVHRR) aboard the National Oceanic and Atmospheric Administration's (NOAA) polar orbiting satellites [Flannigan and Vonder Haar 1986; Kaufman et al., 1990a; Arino and Mellinotte 1998; Justice et al. 1996; Li et al. 1997]. Measurements from many other sensors have also been

employed such as GOES [Menzel et al., 1991; Prins and Menzel, 1994], LANDSAT [Chuvieco and Congalton, 1988], DMSP [Cahoon et al., 1992], ATSR (Arino and Rosaz, 1999), and in the recently launched MODIS (Kaufman et al., 1998a). Each of the instruments has unique advantages and limitations for fire monitoring. For example, GOES offers frequent diurnal sampling (up to every 15 min), allowing a close surveillance of fire development, but at the expense of relatively poor spatial resolution (4 km or coarser) and limited coverage. In contrast, LANDSAT provides much more detailed information on the spatial distribution of individual fires, but suffers from an infrequent revisit (once every 16 days) and very small geographic coverage. It appears that AVHRR aboard NOAA satellites provides a reasonable trade-off between spatial and temporal coverage for global monitoring, with a variety of spectral bands. Besides, the long history of observation and well-understood sensor characteristics make AVHRR the workhorse for many GOFC programs. For example, AVHRR data have been employed to generate the first global fire product for the period April 1992-December 1993 under the IGBP-DIS fire initiative, and are being used to produce a near-real-time global fire data set under the WFW. Reconstruction of fire history over the entire North America is also underway by US and Canadian scientists under NASA's Land Use and Land Cover Change Program, a US contribution to GOFC. A more ideal instrument for fire monitoring is MODIS (onboard the TERRA satellite launched in December 1999) that includes special channels tailored to fire monitoring (Kaufman et al. 1998a). However, MODIS has yet to provide a long-term record of data.

In light of their unique and important role, AVHRR-based fire detection algorithms are the focus of this paper. Algorithms using data from other sensors are discussed in

separate papers in this book. A modified MODIS algorithm adapted to AVHRR data is also discussed, due to its similarity to the AVHRR algorithms. The following section describes the characteristics of AVHRR sensors. Section 3 reviews AVHRR-based fire detection algorithms in terms of their physical principles and limitations. The efficiency and performance of five commonly used algorithms are evaluated by applying them to the Canadian boreal forest (section 4), as a demonstration, which may not be valid for other ecosystems. Section 5 provides general and specific recommendations as to how the algorithms may be improved. A summary and conclusions are presented in the last section.

2. Characteristics of Sensors

To better understand fire detection algorithms, the characteristics of NOAA/AVHRR, as well as EOS/MODIS, are described first. NOAA/AVHRR has two major advantages for fire monitoring. First, the instrument provides daily coverage of the entire planet at a moderate resolution (~1 km), which is critical for operational global fire monitoring. Second, it has wide spectral coverage comprising the visible (ch.1, 0.63 μm), near-infrared (ch.2, 0.83 μm), mid-infrared (ch.3, 3.75 μm), and thermal (ch.4-5, 10-12 μm) wavebands. All channels pertain to certain attributes of fire, but contain different information (Li et al., 1997). Smoke is more discernible in the visible channel, which has been employed to estimate fire smoke and trace gas emissions (Kaufman et al., 1994). However, due to the similar appearance of smoke and clouds in this channel, identification of smoke is better achieved with other AVHRR channels (Li et al. 2000a).

Burned area can be assessed from reflectance differences between the visible and NIR channels (Kasischke et al., 1993; Razafimpanilo et al., 1995; Li et al., 2000b; Fraser et al., 2000), or from indices derived from the NIR/MIR spectral domain (Pereira, 1999; Barbosa et al. 1999). In principle, the size and temperature of sub-pixel fires may be determined from the thermal radiance in two infrared channels (ch. 3 and ch.4) for a uniform background (Dozier, 1981), if the sensor is not saturated and the signal is significant in both channels. In practice, this is often proven to be a difficult task. For example, deforestation fires in South America that are detected by AVHRR increase the signal at 10 μm on average only by 1.5K, which is within the background variability in this channel (Kaufman et al., 1990a). The essence of fire detection lies in significantly enhanced radiance emitted in the mid-infrared region (ch.3) for typical fire temperatures, as governed by the Planck function. The mid-infrared channel is thus most useful for fire detection. It is highly sensitive to the presence of fires, which also poses a problem for fire detection. A very small fire within the 1-km pixel can easily saturate the channel. For example, a fire with a temperature of 1000 K located within a non-reflective background of 300 K, needs only be 13×13 m to saturate the 3.75 μm channel (Kaufman et al., 1990a; Robinson, 1991; Belward et al. 1993). To overcome the problem, channel 4 is often used in combination with channel 3. For moderate resolution satellite data like AVHRR, fires usually have varying temperature within the pixel, rendering unusually large differences in brightness temperature between the two channels.

The MODIS fire detection algorithms are based on those developed for AVHRR, but bring some new capability to the remote sensing arena. In the MODIS design, the 3.75 μm channel was shifted to 3.95 μm to avoid the variable water vapor absorption and

to reduce reflected solar radiation by 40% (Kaufman et al., 1998a). MODIS visible and near IR channels (0.66 and 0.86 μm) both have a resolution of 250 m, which is advantageous for more accurate remote sensing of vegetation and burn scars. MODIS has a 1.65 μm channel (with a resolution of 500 m) that has been shown to be very sensitive to burn scars (Kaufman et al., 1998b; Eva and Lambin 1998). MODIS smoke detection employs the blue (0.41 and 0.47 μm) and mid IR (2.1 μm) channels in addition to the AVHRR red channel (0.66 μm) for better detection and discrimination of smoke from soil dust (Kaufman et al., 1997; Chu et al., 1998).

3. Review of Algorithms: Principles and Limitations

Given that AVHRR fire detection algorithms have been reviewed in several previous papers (Robinson 1991; Justice et al., 1993; Setzer and Malingreau 1996; Martin et al., 1999), the overview given here is brief and focuses more on the physical principles. Similar to the recent classification by Martin et al. (1999), the majority of AVHRR-based fire detection algorithms may be classified in three categories: 1) single channel threshold algorithms based on channel 3; (2) multi-channel threshold algorithms; and 3) contextual algorithms that compare the potential fire pixel with the thermal properties of the background. Note that the single channel and multi-channel threshold algorithms are basically fixed threshold methods, while the contextual ones have variable values of thresholds. There might be a few other types of fire detection algorithms using AVHRR data that are not typical enough to be reviewed here, such as the raw digital count method used operationally in Brazil (Setzer and Pereira, 1991a; Pereira and Setzer, 1993).

3.1 Single-channel threshold algorithm

The single channel threshold algorithms rely only on AVHRR's mid-infrared channel, i.e. channel 3 centered around 3.75 μm. According to the Planck function, emission of thermal radiative energy reaches peak values for typical fire temperatures ranging from 500 K for smoldering fires to over 1000 K for flaming fires (Fig. 1). However, since AVHRR was not designed for fire monitoring, it is saturated at a brightness temperature of 320-331 K (Robinson, 1991), well below the fire temperature. For example, on a background of 300 K, a hot object at 1000 K that occupies only 0.02% of the pixel area can raise the pixel's brightness temperature at 3.75 μm to 324 K. Nevertheless, a non-fire target rarely reaches the saturation point, barring strong reflection of solar radiation due to clouds or bright land. Therefore, the saturated channel 3 is still useful for detecting the presence of fires especially for relatively cool environments and/or regions with low solar reflectivity (Muirhead and Cracknell 1985; Malingreau and Tucker 1988; Setzer and Pereira 1991b, 1992). The single channel threshold algorithm was also applied to other sensors such as the ATSR (Arino, 1999). Single channel thresholding is most useful for the evening satellite overpasses, where the contribution from reflected sunlight is minimal (Malingreau 1990; Langaas 1992).

The most challenging task in using channel 3 to detect fires during daytime is to account for the influence of solar reflection from cloud and bright surfaces within the limits dictated by the low saturation of ch.3. For example, a soil surface with a temperature of 300 K and a reflectance of 0.28 can saturate the 3.75 μm channel, even when no fire is present (Giglio et al. 1999). While fire reflectivity (=1-emissivity) in

channel 3 is very low (almost zero) for fires and decreases with increasing flame depth and intensity (Vines, 1981; Robinson, 1991), the reflectivity of other scene types is not negligible and quite variable (Salisbury and D'Aria, 1994; Giglio et al., 1999). For barren soils, reflectivity in channel 3 ranges from 0.13 to more than 0.4, according to the survey of Setzer and Malingreau (1996) based on the studies of Hovis (1966) and Suits (1989). The relative contribution of this component to the total channel 3 radiance is demonstrated in Fig. 2. It is seen that the reflection of solar radiation plays an increasing role as surface temperature decreases. Solar reflection depends mainly on the amount of incident solar radiation and the albedo. For cos(SZA)=0.8, albedos above 40% can cause channel 3 to saturate. Albedos above 20% can confuse most fire detection algorithms. If the albedo is 5%, solar reflection can never cause the saturation of channel 3 without the presence of a fire. This is the case for the majority of vegetated land, especially forest, which usually has a channel 3 albedo below 5% (Kaufman and Remer, 1994; Giglio et al., 1999; Flannigan and Vonder Haar, 1986). For other types of surface, reflectivity in channel 3 is large and more variable, ranging from 0.14 for winter grassland and tropical savanna to 0.24 for desert (Giglio et al., 1999). The reflectivity of clouds can be even larger and more variable. In view of the above concerns, two recommendations are made to improve the performance of fire detection algorithms intended for application across a range of land cover types:

(1) Screening of bright objects (e.g. cloud, bare surfaces) is applied prior to the use of channel 3 to identify potential fires in order to increase the effectiveness of channel 3 thresholding.

(2) The channel 3 threshold varies according to both land cover type, or more precisely channel 3 reflectivity, and the amount of incoming solar radiation (e.g. use solar zenith angle as a proxy variable).

These recommendations are particularly applicable for detecting fires that are not hot or large enough to cause saturation in channel 3.

3.2 Multi-channel Threshold Algorithms

To overcome some of the difficulties with single channel fire detection, multi-channel threshold algorithms were introduced. The majority of the multi-channel threshold algorithms consist of three basic steps (Kaufman et al. 1990a): (1) use channel 3 to identify all potential fires; (2) use thermal channel 4 to eliminate clouds; and (3) use the difference between brightness temperature in channels 3 and 4 to isolate fires from warm background. Note that these improvements do not correct for the possible presence of reflective surfaces. The multi-channel threshold algorithms were mainly used for regional or even continental applications. So far, they have been applied to detect fires in various biomes such as tropical forest (Kaufman et al., 1990a; Belward et al., 1994); savanna fires in West Africa (Langaas, 1993; Kennedy et al., 1994; Franca et al. 1995); and boreal forests (Cahoon et al., 1991, 1994; Li et al., 1997, 2000c). For each application, thresholds were specifically tuned to cope with unique environmental and fire conditions. In addition to the three basic tests, additional tests may also be applied, in particular for coping with reflective surfaces and different types of clouds. Note that channel 4 is efficient for detecting high cloud decks of cold cloud tops, but it is not

effective for removing low clouds of little thermal contrast with the surface, or residual sub-pixel clouds. Channel 1 visible reflectance measurements have been used to remove low cloud and bright surfaces (Kennedy et al., 1994; Arino, 1998). However among all the AVHRR channels, the visible channel is most susceptible to fire smoke that often accompanies fires, unless it is blown away from fires by strong wind. The channel 2 NIR observation was also used for the same purpose (Li et al., 2000c), which is also affected by smoke but to a substantially lesser degree. Another advantage of using channel 2 is that vegetation albedo diminishes drastically after burning, leaving more contrast with green vegetation. The difference between brightness temperature in channel 4 and 5 (T4-T5) is useful to remove thin cirrus clouds (Inoue, 1987; Franca et al., 1995; Li et al., 1997, 2000c); while the spatial coherence technique proposed by Coakley and Bretherton (1982) was used to exclude sub-pixel clouds (Flannigan and Vonder Haar, 1986).

Among these tests, the T3-T4 test is most efficient in removing false fires, as is shown in later analyses. The test has thus been adopted in all multi-channel threshold algorithms. The common notion is that fire pixels have significantly larger values of T3-T4 than non-burned background. However, the physical basis behind this test is considerably more complex. In principle, four contributing factors could create the T3-T4 difference: (1) unequal atmospheric effects; (2) unequal emissivities; (3) solar reflection in ch.3; and (4) non-uniform fire scenes. Unequal atmospheric effects in the two channels contribute to a difference between T3 and T4, as the transmittance in the two channels is different (Fig. 3). In general, channel 3 is more transparent than channel 4 with corresponding transmittance around 0.9 and 0.75 respectively. On the other hand, atmospheric emission is proportional to the transmission. These offsetting effects of the

atmosphere dampen the difference in the inverted BT. Figure 4 shows the relation between TOA brightness temperatures (T3, T4) and surface blackbody temperature (T). The results were obtained by using the Planck function and a MODTRAN code for a subarctic model summer atmosphere. It follows that (a) both T3 and T4 vary linearly with T and (b) T3-T, T4-T and T3-T4 are usually small for ordinary terrestrial surfaces and increase with T. For T3-T4 to reach a difference of 10 K (a typical threshold used in fire detection algorithms), T needs to be above 370 K and T3 above 363 K. Since channel 3 becomes saturated around 325 K, large differences in T3-T4 could not be incurred by a uniform, hot pixel. On the contrary, hot fires may induce negative values for T3-T4, as the saturation temperature for channel 4 is typically somewhat higher (~330 K). The maximum T3-T4 reachable before T3 saturation (say 325 K) is about 4-5 K. Different emissivities in channels 3 and 4 contribute to the difference in T3-T4, but the contribution is usually minor. Because deserts have quite different emissivities in channels 3 and 4 (0.76 and 0.97 respectively), they can produce negative T3-T4. Moreover, there is no evidence showing that fires have larger differences in emissivities between channels 3 and 4 than background scenes. Solar reflection in channel 3 can cause large T3-T4, but it introduces false alarms rather than helps remove them.

The driving factor causing large T3-T4 differences is the inhomogeneous temperature fields containing fires, as simulated by Dozier (1981) and Kaufman et al. (1998a); and measured by Kaufman et al (1998b). Because of the nonlinear dependence of radiance on temperature, the more heterogeneous the temperature field, the larger the difference in T3-T4 is. This forms the basis for removing false fires when using coarse resolution satellite data such as the 1-km AVHRR data. *This test would not be as effective*

for fine resolution data such as LANDSAT/TM, where fires would frequently cover a large proportion of a pixel. Figure 5 shows the simulation results of T3-T4 against the fraction of fire within a pixel. Only two different temperatures within a pixel are considered: a cool background (300K) and a hot fire whose temperature enhancement is indicated in the plot. T3-T4 is found to reach maximum values for a very small fraction of fire area, mostly well below 0.1. The hotter the fire, the smaller the fraction is required to reach maximum T3-T4. As the fire fraction increases, T3-T4 decreases. If the entire pixel is burning with a uniform temperature, the difference in T3 and T4 vanishes! As such, the use of the T3-T4 difference does not help the detection of large uniform fires.

Giglio et al. (1999) simulated the probability of detection by AVHRR fire algorithms and found that they all miss fires of large fractions ranging from as low as less than 1% to 10% depending on fire temperature and satellite viewing zenith angle (Fig. 6). Use of AVHRR measurements made at large viewing zenith angles reduces this problem, as the fire fraction decreases with increasing field-of-view and pixel size, while there is a concomitant decrease in the probability of detecting small fires. Fortunately, it is rare for a fire to occupy a large proportion of an AVHRR pixel with uniform temperature, as the fire frontier is usually quite narrow. Besides, a fire field usually exhibits rather diverse temperatures that may vary by several hundred degrees (Robinson, 1991). *In the case of large and relative uniform fires, channel 4 could be used to identify fires by setting a higher threshold*, or by examining relative spatial contrast of T4 with respect to its surrounding pixels. For such fires, the commonly used T3 and T3-T4 tests are no longer effective. This problem will be largely eliminated with MODIS fire detection, since the 3.95 μm channel (replacing the AVHRR 3.75 μm channel) is not easily saturated by a

fire, and a simple absolute threshold at 3.95 will detect these large fire with no need for the T3-T4 difference threshold.

3.3 Contextual algorithms

To expand the utility of multi-channel algorithms, multi-channel contextual algorithms were proposed (Lee and Tag, 1990). They were first explored by the IGBP DIS fire working group (Justice and Malingreau 1993) using AVHRR data, and by Prins (1992) using GOES data. The approach was further employed for global and regional fire monitoring (Justice and Malingreau, 1996; Eva and Flasse, 1996; Dwyer et al., 1998), and is now used for the World Fire Web initiative (Gregoire et al. 2000). Instead of using fixed thresholds throughout a study region, a contextual algorithm computes variable, pixel-specific thresholds. This involves two basic steps: initial setting of thresholds to identify potential fire pixels and then fine-tuning the thresholds to confirm fires among the potential fire pixels (Martin et al., 1999). The tests in the first step are similar to the multi-channel threshold techniques except that the thresholds are more liberal to avoid missing real fires. The second step computes the mean and standard deviation of the threshold variables (e.g., T3 and T3-T4, among others) from non-potential fire pixels surrounding a potential fire pixel. The window size for computing the means and standard deviations is set in a somewhat ad-hoc manner, varying typically from 3×3 pixels up to 21×21 (Flasse and Ceccato, 1996) until the number of qualified background pixels reaches a pre-specified value (usually 25% or 3). After obtaining these statistics, they are used to re-define the thresholds to confirm a fire. Giglio et al. (1999) proposed different thresholds for marking initial potential fires and for confirming real fires.

Examples of the threshold settings are presented in section 4. For regional application, there is an advantage to set the thresholds based on regional and seasonal varying surface properties, fuel type and amount, fire strength, etc. (Martin et al., 1999; Chuvieco and Martin, 1994). For global application, a more conservative fire detection algorithm is sometimes desirable. Note that a conservative, global algorithm can be expected to miss many of the smaller fires in an attempt to reduce false fire detection. Therefore such algorithms will be less useful for early fire detection and tactical response. However, these approaches detect the larger fires that are responsible for most of the biomass burning and climate impact. For example, Kaufman et al. (1998b) found that in Brazil, the MODIS algorithm was capable of detecting only 30-40% of the fires, but these fires are responsible for 80-99% of the burned biomass.

4. Evaluation and Inter-comparison of Algorithms and Tests

So far, the discussion has been largely theoretical, while many fire detection algorithms were developed empirically. Both empirical and theoretical algorithms need to be validated thoroughly and extensively, so that the accuracy and limitations of resulting fire products are well documented. While many fire detection algorithms have been proposed, few have been rigorously validated. In most cases, only cursory validations were conducted by comparing against fire smoke plumes. A handful of satellite-based fire studies (e.g. Flannigan and Vonder Haar, 1986; Setzer and Pereira, 1991b; Setzer et al., 1994; Rauste et al., 1997; Li et al., 1997, 2000c) have performed validations using ground-truth information on actual fires. However, such ground-truth

data are severely lacking in most parts of the world. Validation of fire detection algorithms thus remains an acute problem. Apart from validation against ground-truth data, algorithm inter-comparison is also helpful in gaining insight into the performance of the algorithms, at least regarding the consistency among the algorithms under study.

Canada is one of the few countries that maintain a relatively detailed and complete archive of forest fire distribution, allowing evaluation of satellite-based fire detection. In Canada, GIS-based fire polygons showing both the area and spatial distribution of forest fires are produced by provincial and terrestrial fire management agencies using airborne infrared mapping techniques. The Canadian Forest Service (CFS) gathers, compiles, and standardizes the digital fire information and distributes them in GIS format through a National Forestry Database. Such a nation-wide fire inventory data are available for many years. Only the end-of-season (cumulative) burned area polygon data for 1995 are examined here.

4.1 Efficiency of individual tests

Before evaluating the performance of fire detection algorithms, the efficiency of individual fire detection tests that are commonly used is examined. It follows from the above overview that fire detection algorithms exploit information from most of the AVHRR channels. However, these channels do not play equal roles. Li et al. (2000c) examined the relative efficiency of these channels/tests using their multi-threshold algorithm applied over the Canadian boreal forest. The efficiency is measured in terms of the numbers of false fires eliminated (NFF) and real fires retained (NTF) after each test, as is shown in Table 1.

Note that the real fires in the test data set were determined following visual inspections for smoke plumes, and were not confirmed using the CFS fire database. The statistics were derived over a 1000×1000 km^2 region in western Canada. It is clear that use of a channel 3 threshold alone produces a very high proportion of false fires. Although one could increase its threshold to reduce false fires, the number of real fires would also decrease concurrently. Fortunately, the use of series of tests can drastically lower the number of false fires by as much as 98%, but the number of real fires remains largely intact (~10% reduction). The most efficient test for removing false fires is the T3-T4 test, followed by tests based on R2, land cover, etc. Except for the T3-T4 test, relative efficiencies for other tests depend partly on the sequence of implementing the tests. The T4 cloud test appears to be redundant here. However, had the test been applied prior to the R2 test, it would have been much more significant. As far as the boreal forest is concerned, the solar channel shows better contrast than thermal ones between cloudy and clear scenes. It is worth noting that the output shown in Table 1 depends on the algorithm used and the region or season of application, but the conclusions concerning the T3 and T3-T4 may be valid in general. Such an analysis is useful in developing a fire detection algorithm and understanding its performance.

4.2 Evaluation and comparison of the performance of five algorithms

As a demonstration of the utility of inter-comparison exercises, five fire detection algorithms were applied to AVHRR data acquired across Canada. The results from these algorithms are compared to each other and also to the ground-truth data. The analysis serves to 1) characterize the performance of the algorithms in perspective; 2) check the

magnitude of inconsistency among different algorithms; and 3) identify some common problems. Note that the results of the analysis may not be generalized, as they are for a specific ecological and geographical domain. The five algorithms under study include four designed for global applications and one for boreal forest (for details see Table 2). The global algorithms include one used in generating the IGBP-DIS fire product (Malingreau and Justice, 1997), one designed for the MODIS (Kaufman et al., 1998a,b), one employed at the European Space Agency (ESA) (Arino et al., 1998), and one proposed by Giglio et al. (1999). The regional algorithm was developed and is operated at the Canada Center for Remote Sensing (CCRS) (Li et al., 2000b). Two of the algorithms use fixed thresholds (CCRS and ESA) and three use contextual methods with variable thresholds (IGBP, MODIS, and Giglio et al.). All the objective tests in each of the algorithms as listed in Table 2 were implemented. In implementing the three contextual algorithms, the same cloud screening tests were applied following the IGBP, namely, $R1 + R2 \leq 1.2$, $T5 \geq 265$ K, $T5 \geq 285$ K OR $(R1+R2) \leq 0.8$. Pixels passing all these tests are considered to be cloud free. Note that some of the algorithms also include subjective tests (e.g. visual inspection for fire smoke played an important role in eliminating false fires create by the ESA algorithm), which are not included here. Therefore, the results presented here may not be construed as the exact products generated by these algorithms, under the operational structure of the respective organizations using them.

To date, only the IGBP algorithm has been applied at a nearly global scale, including the majority of the earth's biomes. The ESA algorithm was used mainly in the tropics including Africa, South America, and Australia. MODIS was developed for

global operation. Note that the MODIS algorithm was not designed for use with AVHRR data *per se*, but the channels used in MODIS fire detection are sufficiently close to AVHRR channels. On the other hand, since the MODIS fire channel has a much higher saturation temperature and is shifted to a longer wavelength with a smaller contribution of sunlight, its performance as revealed here may be underestimated with respect to what could be realized with actual MODIS data. The algorithm of Giglio et al. (1999) has yet to be applied for global fire detection. While the CCRS algorithm was designed for detecting Canadian boreal forest fires, the thresholds of the algorithm were not tuned against any ground-based fire data. Therefore, the latter data are independent from satellite detection results. The CCRS algorithm was also tested over Russian boreal forest and some temperate regions. During the fire season of 2000, the CCRS algorithm was used to generate daily fire products across both Canada and USA, just a few hours after all images covering these regions were received (ftp://ftp.ccrs.nrcan.gc.ca/ftp/ad/EMS/na_fires/). During the outbreak of fires that occurred in western US states in the summer of 2000, such information played an important role for the Multi-Agency Coordination Group of the Northern Rockies Coordination Center to formulate its daily fire-fighting strategies (Wei-Min Hao, private communication). A preliminary assessment of the quality of the product by the US Forest Service showed similar performance compared to its application in Canada. The algorithm is thus being used to generate historical forest fire products across the continent of North America dating back to 1985 as a project of the NASA LCLUC program.

The main findings of the analysis are summarized below, while a detailed analysis will be presented in a separate paper (Ichoku et al., 2000):

- The spatial distribution of fire hot spots across Canada is similar among the algorithms under study, but the commission and omission errors differ significantly (Fig. 7). The CCRS algorithm was designed for boreal forest applications and thus provides superior overall performance in terms of trade-off between omission and commission errors (Fig. 7)**.** Most of the hot spots detected by the CCRS algorithm fall within the CFS's fire polygons and some of those outside the polygons are verified to be real fires not mapped by provincial and territorial fire agencies (Fraser et al. 2000). Fires missed by the CCRS algorithm are mainly obscured by cloud. The commission error is quite low, but not the lowest among the algorithms. The lowest commission error results from the MODIS algorithm, which occurs at the expense of missing a significant number of real fires. Other global algorithms also demonstrate trade-off between omission and commission errors. Similar to MODIS, the ESA algorithm is quite conservative, and also produces very few false fires. By contrast, the IGBP algorithm is too liberal with the highest level of commission error, but a low rate of omission error. The Giglio et al. algorithm results lie somewhere in between, with moderate omission and commission errors. In short, the results of fire detection with these leading algorithms are far from consistent in terms of numbers, but agree reasonably well in terms of the spatial pattern of fire distribution. Overall, no existing fire detection algorithm will likely perform optimally across a range of biomes and environments.

- All algorithms suffer significant, but varying levels of commission error over the agricultural region in the Canadian western prairies (Fig. 8). Solar reflection from bare soil is thought to be the major cause, as many of the false alarms occurred

in late May and June when snow cover is gone but vegetation (mainly crops and grassland) has not greened up enough to cover the bare soil. Soil has much larger reflectivity than green foliage, as observed by Salisbury and D'Aria (1994) who made extensive observations of emissivity for a large variety of terrestrial materials around the spectral region of AVHRR channel 3. The minimum, maximum, and mean values for many types of rocks, soil, and vegetation are computed from their tabulated data and plotted in Fig. 9. Note that the dominant soil types in the western prairies are Mollisols and Aridisols whose reflectivity in channel 3 are up to ten times that of green foliage, which can easily cause confusion in all of the algorithms under consideration.

- A correlation analysis was performed between the number of fire pixels detected daily by each of the five algorithms throughout Canada, regardless of whether they represent true or false fires, during the period 01 May to 31 October 1995. The result is shown in Table 3. Overall, there are strong correlations between the number of pixels detected by the algorithms. ESA is very closely correlated with CCRS because they are both multi-channel fixed-threshold algorithms. All the contextual algorithms are related to the CCRS algorithm by approximately the same amount. On the other hand, the largest correlation exists between ESA and MODIS algorithms because of their strict fixed thresholds, and because the contextual thresholds used by MODIS are also strict for AVHRR data, and seldom applied in the cases observed.

It should be noted that a potential bias exists as a result of the validation method employed in this preliminary analysis (i.e. comparison of cumulative hot spots to *end-of-*

season burned area polygons). Specifically, any false alarms occurring within the CFS fire polygons will be misinterpreted as successfully detected active fire pixels, increasing the apparent detection rate. One potentially significant source of false alarms within these polygons are sub-regions burned earlier in the burning season, which are generally characterized by more exposed soil, less vegetation, and the presence of ash. The resulting change in land cover may induce false alarms, especially among the contextual algorithms.

This phenomenon is clearly evident for the IGBP algorithm, which exhibited clusters of false alarms within several areas burned during the previous year (1994) (Li et al., 2000b). The most prominent of these occur in the upper center and lower left of the forested area shown in Fig. 7. It is likely that some of the 1995 hot spots were in fact burned (rather than burning) areas as well.

5. Recommendations for Algorithm Improvement

Although the findings discussed in the last section should be considered in the context of a regional application, it is safe to conclude that the performance of existing fire detection algorithms differs drastically. As a result, the quality of fire products generated from a single algorithm applied across various ecosystems may need considerable enhancement to meet the needs of user communities. To some extent, quality deficiencies originate from numerous inherent technology limitations such as low frequency of satellite overpass, poor spatial resolution, sensor saturation, etc. that may not be resolved by means of R&D on algorithm development. On the other hand, *the*

potential capabilities of current space-borne observation technologies have not been fully explored. In principle, the quality of fire products may be improved significantly by more R&D studies on identification of algorithm limitations, and innovation and improvement of algorithms. The drastic discrepancies among the algorithms evaluated above underscore the potential for algorithm improvement on a regional basis.

During the GOFC fire workshop, many discussions took place on the improvement of fire detection algorithms, some of which are outlined here. To improve an algorithm, its limitations must be identified first through extensive validation against ground-truth data sets as well as algorithm inter-comparison. Given the severe lack of ground-truth information, it is recommended that more field campaigns and operational air-borne fire monitoring exercises be conducted. Meanwhile, efforts are needed to identify and explore the utility of *all* existing ground-truth data sets. Validation using high-resolution satellite data sets such as LANDSAT 7 is a sound alternative. As demonstrated above, algorithm inter-comparison is instrumental in identifying the range and source of uncertainties, which may be carried out for different ecosystems and sensors. The following specific recommendations help solve some individual algorithm problems:

1) setting thresholds based on land cover type, or reflectivity/emissivity;
2) replacing threshold approaches by physical models;
3) development of innovative algorithms to take advantage of multi-sensor capability offered by future satellite observations;
4) explore the utility of time series of images.

In developing and improving fire detection algorithms, one should also bear in mind the needs of different user groups. For climate research community, relatively speaking,

the efficiency of running a detection algorithm is secondary to its accuracy, while for fire management community both accuracy and processing speed are key. To date, more emphasis has been placed on the development of fire detection algorithm for the sake of climate change studies. Relatively less R&D efforts were tailored to meeting the needs of a much larger user group, namely, the general public and fire management agencies. To satisfy their needs, fire detection algorithms are required to be *robust, fast, accurate, and automatic*. The algorithms should have very low rates of commission and omission errors, especially the latter. Little or no human supervision may be involved in running such algorithms.

6. Summary and Concluding Remarks

This paper presents an overview of fire detection algorithms designed primarily for use with AVHRR data, except one adapted for use with MODIS data. Emphasis of the review is placed on the physical principles, limitations, and potential improvement of the algorithms. Two major types of algorithms are dealt with in more detail, namely, the multi-channel threshold methods and the spatial contextual methods. In principle, the contextual methods are more versatile for application to a wide range of conditions than the fixed threshold approaches, but a threshold approach may provide more accurate results if it is specifically tailored for application to a particular region/biome. The most serious problems suffered by both types of algorithm are caused by the saturation of channel 3 and its contamination by solar reflection. Both problems are anticipated to be resolved or lessened by the MODIS sensors due to the inclusion of a special fire channel

(3.9 μm instead of 3.7 μm) that has a wider dynamic range and is less influenced by solar reflection. There remain several outstanding issues for AVHRR-based fire detection. The most challenging is to account for the contribution of solar radiation due to reflection from cloud and earth's surfaces. The majority of the algorithms include cloud screening tests that are reasonably efficient in removing false alarms by clouds, but few algorithms are capable of eliminating false alarms caused by surface reflection. This leads to a high rate of commission error over bare land surfaces by the majority of fire detection algorithms. To overcome the problem, it is recommended to either screen out bright surfaces (in channel 3 wavelengths) or to specify the threshold according to land cover types, or more precisely surface reflectivity/emissivity, and to the amount of incoming solar radiation.

Due to the importance of the T3-T4 test in multi-threshold detection algorithms, a further insight was gained into the physical principles and limitations associated with this test. While it was often stated in the literature that the test helps distinguish fire hot spots from warm background, it is underlined here that the test only works for thermally inhomogeneous pixels, regardless of the mean scene temperature itself. Although there are many factors affecting the T3-T4 difference, each of which was investigated, only thermal inhomogenity has a positive and significant contribution to large differences in T3-T4 associated with fires. When there is temperature variability within a satellite's instantaneous field of view (IFOV) or pixel, radiance emitted from the burning portion of the IFOV is much larger in channel 3 than in channel 4, whereas their difference in radiance from the non-burned area is much smaller. The total radiance received by a sensor is a linear combination of separate radiances weighted by their areas. Therefore,

when the total radiance is converted into brightness temperature using the non-linear Planck function, the difference between the two channels is proportional to the thermal inhomogenity of the observed scene. Fortunately, most fire events are non-uniform at the AVHRR pixel size, making this test effective in removing the majority of the false fire alarms.

For the contextual algorithms, the selection of initial thresholds for identifying potential fire pixels is delicate. An overly high setting leads to large omission errors, as the confirmation tests are only limited to potential fire pixels. On the other hand, an overly low setting introduces too much noise in determining the statistics for the background. Most of the contextual algorithms employed fixed and identical thresholds to identify potential fire pixels and the background non-fire pixels. Considering the different functions and consequences of threshold settings, it is recommended that more liberal thresholds be used to identify potential fire pixels and more conservative thresholds be used to calculate non-fire background statistics. Since the severity of a fire varies considerably with fuel type, fuel amount, and weather conditions, the thresholds should also be contingent upon these variables. As a first approximation, one may use different thresholds over different land cover types in different seasons, or set the threshold as a function of a vegetation index.

While a lot of fire detection algorithms have been employed to generate fire products, the products still encompass much shorter periods and smaller areas than are potentially available from satellite. For example, the global IGBP fire product was generated for 20 months (1992-1993) only. An operational near-real time fire product providing global coverage became available only recently from the World Fire Web

network. Longer-term operational fire products are available in very limited countries such as in Brazil and Canada (7 years). However, increasing efforts are being made to produce much more comprehensive fire products from AVHRR. NOAA's archive of 1-km AVHRR data dating back to 1985 is being explored to generate a historical fire data base across North America's forests. Many efforts are also being undertaken in other countries, especially in Europe to generate both near-real-time and historical fire products. It is envisioned that before long we will encounter multiple fire products over the same region/period. Evaluation of the quality of these products becomes a more challenging issue than generating them, which is tied directly to the quality of fire detection algorithm.

Acknowledgment: The views and comments expressed in this paper originated not only from the authors of the article, but also from the fire community at large, especially the participants of the GOFC Fire Workshop held at the Joint Research Centre in Italy 1999. We are particularly grateful to F. Ahern, C. Justice, J.-M. Gregoire for their leadership and dedication to the GOFC fire program, which made this publication possible.

References

Ahern F. , Janetos A. C. , and E. Langham, Global Observation of Forest Cover: One Component of CEOS' Integrated Global Observing Strategy. Proceedings of the 27th International Symposium on Remote Sensing of Environment, Tromso, Norway, June 8-12, 1998.

Ahern, F., GOFC: Goals, status, the fire component and its relationship to the CEOS carbon theme, this publication, 2000.

Arino, O., and J.M. Mellinotte, The 1993 Africa fire map, *Int. J. Rem. Sens*., 19:2019-2023, 1998.

Arino, O., and J-M. Rosaz, 1997 and 1998 World ATSR Fire Atlas using ERS-2 ATSR-2 Data. Proceedings of the Joint Fire Science Conference, Boise, 15-17, June 1999.

Barbosa, P.M., J.-M. Gregoire, and J.M.C. Pereira, An algorithm for extracting burned areas from time series of AVHRR GAC data applied at continental scale, *Rem. Sens. Environ*., 69:253-263, 1999.

Belward, A.S., P.J. Kennedy and J.M. Gregoire, The limitation and potential of AVHRR GAC data for continental scale fire studies, *Int. J. Rem. Sens.*, 15:2215-2234, 1994.

Belward, A.S., J.-M. Gregoire, G. D'Souza, S. Trigg, M. Trigg, M. Hawkes, J.-M. Serca, J.-L. Tireford, J.-M. Charlot, R. Vuattoux, In situ, real time fire detection using NOAA/AVHRR data, Proceedings of the VI AVHRR Data User's Meeting,

Belgirate, Italy, 29th June – 2nd July 1993, published by EUMETSAT, Darmstadt, Germany, EUM P 12, ISSN 10159576, 333-339, 1993.

Cahoon, D.R., Jr., J.S. Levine, P. Minnis, G.M. Tennille, T.W. Yip, P.W. Heck, and B.J. Stocks, The Great Chinese Fire of 1987: *A View from Space, Global Biomass Burning: Atmospheric, Climate, and Biospheric Implications*, J.S. Levine, editor, MIT Press, Cambridge, MA, 61-66, 1991.

Cahoon, D.R., Jr., B.J. Stocks, J.S. Levine, W.R. Cofer III, K.P. O'Neill, Seasonal distribution of African savanna fires, *Nature*, 359:812-815, 1992.

Cahoon, D.R., Jr., B.J. Stocks, J.S. Levine, W.R. Cofer, and J.M. Pierson, Satellite analysis of the severe 1987 forest fires in northern China and southeastern Sibera, *J. Geophys. Res*., 99:18627-18638, 1994.

Chu, A., Y. J. Kaufman, L. A. Remer, B. N. Holben: Remote sensing of smoke from MODIS Airborne Simulator During SCAR-B Experiment. *J. Geophys. Res.,* 103: 31,979-31,988, 1998.

Chuvieco, E., and R.G. Congalton, Mapping and inventory of forest fires from digital processing of TM data, *Geocarto International, 3*:41-53,1988.

Chuvieco, E., and M.P. Martin, A simple method for fire growth monitoring using AVHRR channel 3 data, *Int. J. Rem. Sens*., 15: 3141-3146, 1994.

Coakley, Jr, J.A. and F.P. Bretherton, Cloud cover from high-resolution scanner data: detecting and allowing for partially filled fields of view, *J. Geophy. Res*., 87:4917-4932, 1982

Crutzen, P.J., L.E. Heidt, J.P. Krasnec, W.H. Pollock, and W. Seiler, Biomass burning as a source of atmospheric gases, CO, H_2O, N_2O, NO, CH3CL and COS, *Nature, 282*: 253-256, 1979.

Crutzen, P.J., and M.O. Andreae, Biomass burning in the tropics: Impact on atmospheric chemistry and biogeochemical cycle, *Science*, 250:1669-1678, 1990.

Dozier, J., A method for satellite identification of surface temperature fields of subpixel resolution, *Rem. Sen. Environ.,* 11:221-229, 1981.

Dwyer, E., J.-M. Gregoire, and J.-P. Malingreau, A global analysis of vegetation fires using satellite images: Spatial and temporal dynamics, *Ambio*, 27:175-181, 1998.

Eva, H., and S. Flasse, Contextual and muliple-threshold algorithms for regional active fire detection with AVHRR data, *Rem. Sens. Rev*., 14:333-351, 1996.

Eva, H.D., and E. Lambin, Burnt area mapping in central Africa using AATSR data*, Int. J. Rem. Sens*., 18:3473-3497, 1998.

Flannigan, M.D., and T.H. Vonder Haar, Forest fire monitoring using NOAA satellite AVHRR, *Can. J. Forest Res.,* 16:975-982, 1986.

Flasse, S.P., and P. Ceccato, A contextual algorithm for AVHRR fire detection, *Int. J. Rem. Sens.*, 17:419-424, 1996.

Franca, J.R, J.M. Brustet, J. Fontan, Multispectral remote sensing of biomass burning in West Africa, *J. Atmos. Chem*., 22:81-110.

Fraser, R.H., Li, Z., and Cihlar, J., Hotspot and NDVI Differencing Synergy (HANDS): a new technique for burned area mapping over boreal forest. *Rem. Sens. Environ.,* In Press, 2000.

Giglio, L., J.D. Kendall, and C. O. Justice, Evaluation of global fire detection using simulated AVHRR infrared data, *Int. J. Rem. Sens*., 20:1947-1985, 1999.

Grégoire J-M., D. R. Cahoon, D. Stroppiana, Z. Li, S. Pinnock, H. Eva, O. Arino, J.M. Rosaz, and I. Csiszar, Forest fire monitoring and mapping for GOFC: current products and information networks based on NOAA-AVHRR, ERS-ATSR, and SPOT-VGT, *Rem. Sens. Environ*., this publication, 2000.

Hovis, W.A. Jr. Infrared spectral reflectance of some common minerals, *Apl. Opt*., 5:245-248, 1966.

Ichoku, C., Y. Kaufman, L. Giglio, Z. Li, R. Fraser, J.-Z. Jin, B. Park, Comparative analysis of daytime fire detection algorithms using AVHRR data for the 1995 fire season in Canada: Perspective for MODIS. In preparation, 2000.

Inoue, T., 1987, A cloud type classification with NOAA-7 split-window measurements, *J. Geophy. Res.*, 92: 3991-4000.

Justice, C., J.P. Malingreau, A.W. Setzer, Remote sensing of fires: Potential and limitations, *Fire in the Environment* (P.J. Crutzen and J.G. Goldammer, Eds.), pp. 77-88, 1993.

Justice, C., and J.P. Malingreau (editors), *Report of the IGBP-DIS fire algorithm workshop 2*, IGBP-DIS working paper 14, Ispra, Italy, October 1995, 1996.

Justice, C.O., Kendall, J.D., Dowty, P.R., Scholes, R.J., Satellite remote sensing of fires during the SAFARI campaign using NOAA advanced very high resolution radiometer data, *J. Geophy. Res*, 101: 23851-23863,1996.

Justice, C.O., and J.P. Malingreau (editors), *The IGBP-DIS Satellite Fire Detection Algorithm Workshop Technical Report*, IGBP-DIS Working Paper 9, NASA/GSFC, Greenbelt, Maryland, USA, February, 1993.

Kasischke, E.S., N.H.F. French, P. Harrell, N. Christensen, Jr., S.L. Ustin, D. Barry, Monitoring of wildfires in boreal forests using large area AVHRR NDVI composite image data, *Rem. Sen. Environ.,* 45:61-71, 1993.

Kaufman, Y. J. and R. S. Fraser, 1997: The effect of smoke particles on clouds and climate forcing, *Science*, 277, 1636-1639.

Kaufman, Y.J., C. Justice, L. Flynn, J. Kendall, E. Prins, D.E. Ward, P. Menzel, and A. Setzer, Potential global fire monitoring from EOS-MODIS, *J. Geophy. Res*., 103:32215-32238, 1998a.

Kaufman, Y. J., R. G. Kleidman, M. D. King: SCAR-B Fires in the Tropics: properties and their remote sensing from EOS-MODIS. *J. Geophys. Res.*, 103:31,955-31,969, 1998b.

Kaufman, Y. J., D. Tanré, L. Remer, E. Vermote, A. Chu, and B. N. Holben, Remote Sensing of Tropospheric Aerosol from EOS-MODIS Over the Land Using Dark Targets and Dynamic Aerosol Models. *J. Geophys. Res.*, 102:17051-17067, 1997.

Kaufman, Y. J., L. Remer, Detection of forests using mid-IR reflectance: An application for aerosol studies. *IEEE J. Geosc. Rem. Sens.*, 32:672-683, 1994.

Kaufman, Y.J., D. Tanre, and D.E. Ward, Remote sensing of biomass burning in the Amazon, *Rem. Sens. Rev*., 10: 51-90, 1994.

Kaufman, Y.J., C.J. Tucker, I. Fung, Remote sensing of biomass burning in the tropics, *J. Geophy. Res*., 95: 9927-9939, 1990a.

Kennedy, P.J., Belward, A.S., Gregoire, J.-M., An improved approach to fire monitoring in West Africa using AVHRR data, *Int. J. Remote Sens*, 15:2235-2255, 1994.

Langaas S., Temporal and spatial distribution of Savannah fires in Senegal and the Gambia, West Africa, 1989-90, derived from muilti-temporal AVHRR night images. *Int. J. Wildland Fire*, 2: 21-36, 1992.

Langaas S., A parameterised bispectral model for savanna fire detection using AVHRR night images, *Int. J. Remote Sens*., 14:2245-2262, 1993.

Lee, T.M., and P.M. Tag, Improved detection of hotspots using the AVHRR 3.7 um channel. *Bull. Amer. Meteoro. Soc*. 71**:**1722-1730, 1990

Li, Z., H. Barker, and L. Moreau, The variable effect of clouds on atmospheric absorption of solar radiation, *Nature*, 376**,** 486-490, 1995.

Li, Z., Influence of absorbing aerosols on the solar surface radiation budget, *J. Climate*, 11:5-17, 1998.

Li, Z., Cihlar, J., Moreau, L., Huang, F., Lee, B., Monitoring fire activities in the boreal ecosystem, *J. Geophy. Res.*, 102:29611-29624, 1997.

Li, Z., A. Khananian, R. Fraser, Detecting smoke from boreal forest fires using neural network and threshold approaches applied to AVHRR imagery, *IEEE Tran. Geosci. & Rem. Sen.,* revised, 2000a.

Li, Z., S. Nadon, J. Cihlar, B. Stocks, Satellite mapping of Canadian boreal forest fires: Evaluation and comparison of algorithms *Int. J. Rem. Sens*., 21:3071-3082, 2000b.

Li, Z., S. Nadon, J. Cihlar, Satellite detection of Canadian boreal forest fires: Development and application of an algorithm, *Int. J. Rem. Sens*., 21:3057-3069, 2000c.

Malingreau, J.P., The contribution of remote sensing to the global monitoring of fires in tropical and sub-tropical ecosystems. In: *Fire in the Tropical Biota*, edited by J.G. Goldammer, pp. 337-370. Berlin: Springer-Verlag, 1990.

Malingreau J.P. and C.J. Tucker, Large scale deforestation in the south-eastern Amazon basin. *Ambio*, 17: 49-55, 1988.

Malingreau, J.P. and Justice, C.O., (editors), *The IGBP-DIS Satellite Fire Detection Algorithm Workshop Technical Report*, IGBP-DIS Working Paper 17, NASA/GSFC, Greenbelt, Maryland, USA, February, 1997.

Martin, P., Ceccato, P., Flasse, S., and Downey, I. Fire detection and fire growth monitoring using satellite data. Remote Sensing of Large Wildfires in the European Mediterranean Basin, Chuvieco, E., (Ed.). Springer-Verlag Berlin/Heidelberg 3-540-65767-3, XII, 212 pp, 1999.

Matson, M., G. Stephens, and J. Robinson, Fire detection using data from the NOAA-N satellites, *Int. J. Rem. Sens*., 8:961-970, 1987.

Menzel, W.P., E.C. Cutrim, and E.M. Prins, Geostationary satellite estimation of biomass burning in Amazonia during BASE-A, *Global Biomass Burning* (J.S. Levine, Ed), MIT Press, Cambridge, MA, 41-46, 1991.

Muirhead, K. and A. Cracknell, Straw burning over Great Britain detected by AVHRR, *Int. J. Rem. Sens.*, 6: 827-833, 1985.

Pereira, M.C., and A.W. Setzer, Spectral characteristics of deforestation fires in NOAA/AVHH images, *Int. J. Rem. Sens*., 14:583-597, 1993.

Pereira, J.M.C., A comparative evaluation of NOAA/AVHRR vegetation indexes for burned surface detection and mapping. *IEEE Trans. Geosci. Remote Sens*. 37:217-226, 1999.

Prins, E.M., and W.P. Menzel, Trends in South American biomasss burning detected with the GOES VISSR radiometer atmospheric sounder from 1983 to 1991, *J. Geophy. Res*., 99:16719-16735, 1994.

Prins, E.M. and W.P. Menzel, Geostationary satellite detection of biomass burning in South America. *Int. J. Remote Sensing,* 13:2783-2799, 1992.

Rauste, Y., E. Herland, H. Frelander, K. Soini, T. Kuoremaki, and A. Ruokari, Satellite-based forest fire detection for fire control in boreal forests, *Int. J. Rem. Sens*., 18:2641-2656, 1997.

Razafimpanilo, H., R. Frouin, S.F. Iacobellis, and R.C.J. Somerville, Methodology for estimating burned area from AVHRR reflectance data, *Rem. Sen. Environ.,* 54:273-289, 1995.

Reid JS, Hobbs PV, Rangno AL, Hegg DA Relationships between cloud droplet effective radius, liquid water content, and droplet concentration for warm clouds in Brazil embedded in biomass smoke, 104, 6145-6153, 1999.

Robinson, J.M., Fire from space: Global fire evaluation using infrared remote sensing, *Int. J. Rem. Sen*., 12:3-24, 1991.

Salisbury, J.W., and D.M. D'Aria, Emissivity of terrestrial materials in the 3-5 μm atmospheric window, *Rem. Sens. Envion*., 47:345-361, 1994.

Setzer A.W., and M.C. Pereira, Operational detection of fires in Brazil with NOAA-AVHRR, *24th Symp. Rem. Sens. Environ.*, Rio de Janeiro, Brazil, May 1991a.

Setzer, A.W. and M.C. Pereira, Amazonian biomass burnings in 1987 and an estimate of their tropospheric emission, *Ambio* 20, 19-22, 1991b.

Setzer, A.W. and M.C. Pereira, Operational detection of fires in Brazil with NOAA-AVHRR. Proc. 24th *Int. Symp. Remote Sensing of the Environ.*, pp 469-482, Rio de Janeiro, 1992.

Setzer, A.W., M.C. Pereira, and Jr.A.C. Pereira, Satellite studies of biomass burning in Amazonia - some practical aspects. *Rem. Sens. Rev.*, 10:91-103, 1994

Setzer, A.W. and Malingreau, J.P., AVHRR monitoring of vegetation fires in the tropics: Toward the development of a global product. *Biomass Burning and Global Change*, (ed. J.S. Levine), p. 25-39, The MIT Press, Cambridge, Massachusetts, London, England, 1996.

Suits, G.H., Natural Sources, in The Infrared Handbook, Ed. W.L. Wolfe and G.J. Zissis, MI, pp. 3.1-3.154 (Ann Arbor, E.R.I.M.), 1989

Vines, R.G., Physics and chemistry of rural fires, In *Fire and the Australian Biota*, edited by A.M. Gill, R.H. Groves and I.R. Noble, Canberra: Australian Academy of Science, pp129-151, 1981.

Table 1. Summary of the fire-detection tests and the statistics of their efficiency (after Li et al. 2000a). NTF and NFF are the numbers of true and false fires remained after each step of detection tests, respectively.

Test #	Description	Threshold	NTF	NFF
1	Initial test	T3 > 315K	12 569	168168
2	Eliminate warm background	T3-T4 >14K	12 569	48855
3	Eliminate non-forest scenes	Land cover	12 569	30 511
4	Eliminate bright scenes	R2 < 0.22	12 442	5 665
5	Eliminate cloud edges or thin clouds	T4-T5>4.1K T3-T4<19K	11 307	2 673
6	Eliminate cold clouds	T4<260K	11 307	2 673
7	Eliminate single fire pixels		11 160	1 828

Table 3. Correlations between the hot spots detected by various algorithms.

	CCRS	*ESA*	*GIGLIO*	*IGBP*	*MODIS*
CCRS	1.00				
ESA	0.91	1.00			
GIGLIO	0.80	0.81	1.00		
IGBP	0.82	0.70	0.80	1.00	
MODIS	0.81	0.94	0.77	0.62	1.00

Table 2. Five fire detection algorithms tested over the Canadian boreal forest. Note that all statistics (av, ad, md, sd) refer to background pixels; all temperature values are expressed in degrees Kelvin (K); all thresholds given here refer to daytime data.

Algorithm / Description	**CCRS**	**ESA**	**IGBP**	**GIGLIO**	**MODIS**
Algorithm category and geographic applicability	fixed thresholds, regional (Canada)	fixed thresholds, global/regional	contextual, global	contextual, global	contextual, global
Potential fire detection			T_3>311 AND T_{34}>8	T_3 >310 AND T_{34}>6	T_3 ≥315 AND T_{34}≥5
Background window size			3x3 to 15x15	5x5 to 21x21	3x3 to 21x21
Min. number of pixels			Max{25% of pixels tested , 3}	Max{25% of pixels tested , 6}	Max{25% of pixels tested , 3}
Background selection			T_3≤311 OR T_{34}≤8	T_3≤318 OR T_{34}≤12	T_3≤320 OR T_{34}<20
Actual fire detection with T_3 and/or T_4	T_3>315	T_3>320	Define: ξ_3= av(T_3)+2*sd(T_3)+3 ξ_{34}= Max{8, av(T_{34})+2*sd(T_{34})} Then, Confirm potential fires as real if: $T_3 > \xi_3$ AND $T_{34} > \xi_{34}$	Define: ξ_4= av(T_4) + ad(T_4) - 3 ξ_{34}= av(T_{34})+Max{2.5*ad(T_{34}),4} Then, Confirm potential fires as real if: $T_4 > \xi_4$ AND $T_{34} > \xi_{34}$	Define: ξ_3=Min[320,av(T_3)+4*Max{sd(T_3),2}] ξ_{34}=Min[20,md(T_{34})+4*Max{sd(T_{34}),2}] Then, Confirm potential fires as real if: T_3>360 OR [T_3>ξ_3 AND T_{34}>ξ_{34}]
Filter hot surfaces	T_{34}≥14	T_{34}>15	Incorporated into fire detection	Incorporated into fire detection	Incorporated into fire detection
Filter clouds	T_4≥260	T_4>245	R_1+R_2≤1.2 AND T_5≥265 AND (R_1+R_2≤0.8 OR T_5≥285)	*IGBP criteria applied here (no external cloud mask).*	*IGBP criteria applied here (no external cloud mask).*
Filter reflective surfaces	R_2≤0.22	R_1<0.25	R_2<0.20	R_2<0.25	
Filter sun glint		|R_1-R_2|>0.01			R_1≤0.3 OR R_2≤0.3 OR reflected sun angle ≥ 40^o
Other detection criteria	T_{34}≥19 OR T_{45}<4.1				
Post processing (*not applied in this investigation*)	• Elimination of non-forest and isolated pixels	• Quicklook inspection, • Max annual NDVI > 0			

TABLE 2 Footnote

R_1 = Reflectance in Band 1 (0.66 μm)
R_2 = Reflectance in Band 2 (0.86 μm)
T_3 = Brightness Temperature in Band 3 (3.75 or 3.95 μm for MODIS)
T_4 = Brightness Temperature in Band 4 (10.8 μm)
T_5 = Brightness Temperature in Band 5 (11.9 μm)
$T_{34}=T_3-T_4$
$T_{45}=T_4-T_5$
av( ): mean; ad( ): mean absolute deviation
md( ): median, sd( ): standard deviation

Figure Captions

Figure 1. Plank function and the locations of AVHRR channels 3 and 4 (modified after Matson et al., 1987)

Figure 2. Relationship between Ch. 3 brightness temperature and surface temperature with varying contribution of solar reflection. The brightness temperatures are inverted from radiances as computed by $R_3 = \alpha S_0 \mu_0 / \pi + (1-\alpha) B(\lambda_3, T_b)$, where S_0 is Ch.3 solar constant, μ_0 is cos SZA, α is albedo, λ_3 is effective Ch.3 wavelength, T_b is surface temperature. Atmospheric attenuation is neglected. The upper and lower panels show the influence of albedo and solar zenith angle.

Figure 3. Atmospheric transmittances (solid curves) in the spectral regions of AVHRR channels 3 and 4 computed by MODTRAN3.7 for the sub-Arctic summer atmosphere. The radiometer's spectral response functions are also shown in the figure.

Figure 4. Relationships between the brightness temperature at the top of the atmosphere and the surface temperature in AVHRR channels 3 and 4. Atmospheric effects are accounted for by the MODTRAN 3.7 code that computes atmospheric attenuation due to absorption and enhancement due to emission.

Figure 5 Difference between AVHRR channels 3 and 4 TOA brightness temperatures as a function of the fraction of a fire whose temperature exceeds background temperature by an amount ranging from 100K to 800K.

Figure 6. Fire detection envelop at scan angles of 0^{o}(a), 40^{o}(b) and 55^{o}(c) using the ESA algorithm (Arino et al. 1993) for fires in the tropical rain forest biome (From Giglio et al. 1999).

Figure 7. Comparison of fire hot spots detected by the five algorithms against fire polygons obtained by Canadian forest agencies.

Figure 8. Comparison of fire detection results by the five algorithms over the Canadian prairies.

Figure 9. Mean, minimum and maximum values of the reflectivity in AVHRR channel 3 observed for many samples of soils (top) and vegetation (bottom) (reproduced from Salisbury and D'Aria, 1994).

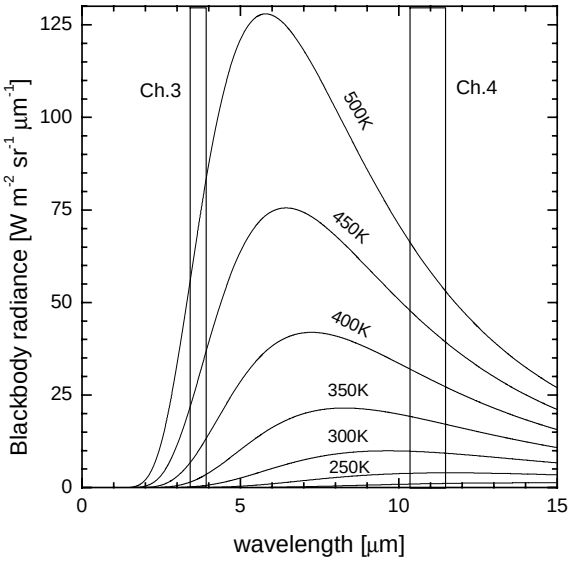

Figure 1. Plank function and the locations of AVHRR channel 3 and 4.

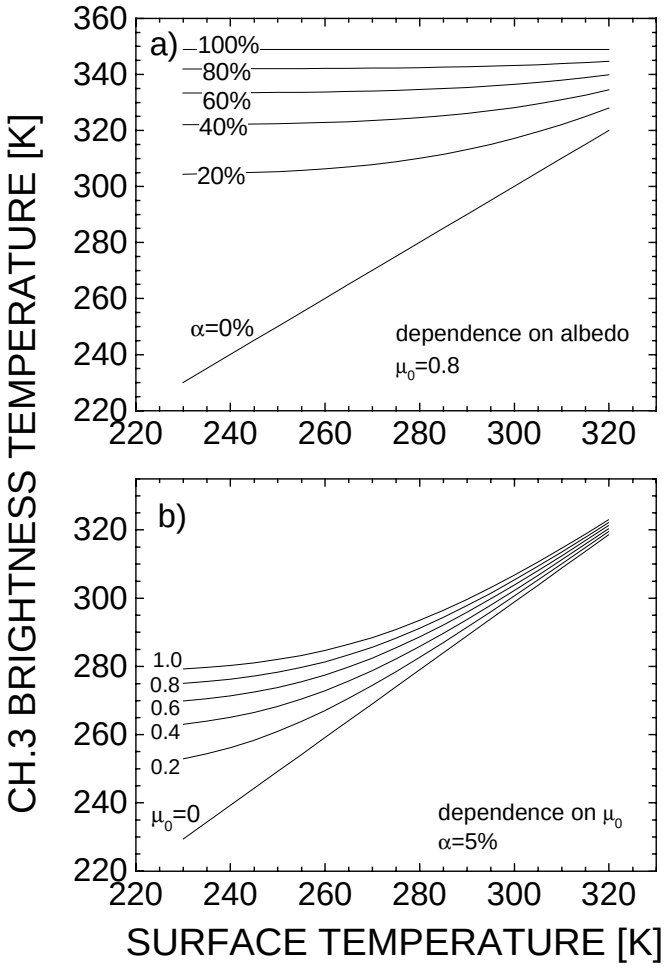

Figure 2. Relationship between Ch. 3 brightness temperature and surface temperature with varying contribution of solar reflection. The brightness temperatures are inverted from radiances as computed by $R_3 = \alpha S_0 \mu_0 / \pi + (1-\alpha) B(\lambda_3, T_b)$, where S_0 is Ch.3 solar constant, μ_0 is cos SZA, α is albedo, λ_3 is effective Ch.3 wavelength, T_b is surface temperature. Atmospheric attenuation is neglected. The upper and lower panels show the influence of albedo and solar zenith angle.

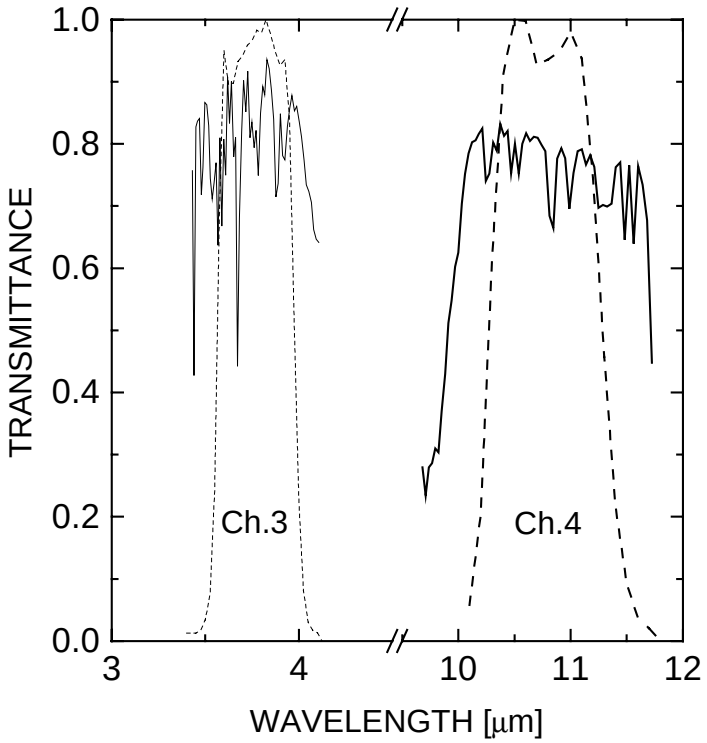

Figure 3. Atmospheric transmittances (solid curves) in the spectral regions of AVHRR channel 3 and 4 computed by MODTRAN3.7 for the sub-Arctic summer atmosphere. The radiometer's spectral response functions are also shown in the figure.

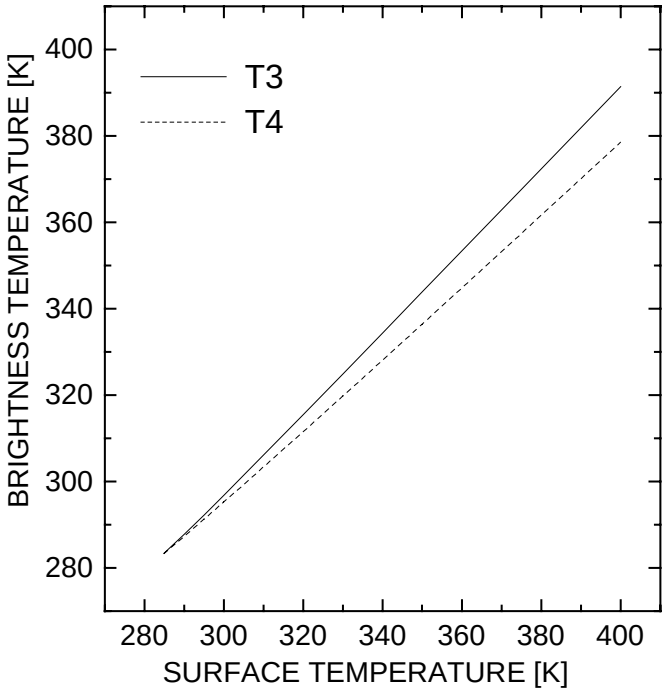

Figure 4. The relationships between brightness temperature at the top of the atmosphere and surface temperature in AVHRR channel 3 and 4. Atmospheric effects are accounted for by the MODTRAN 3.7 code that computes atmospheric attenuation due to absorption and enhancement due to emission.

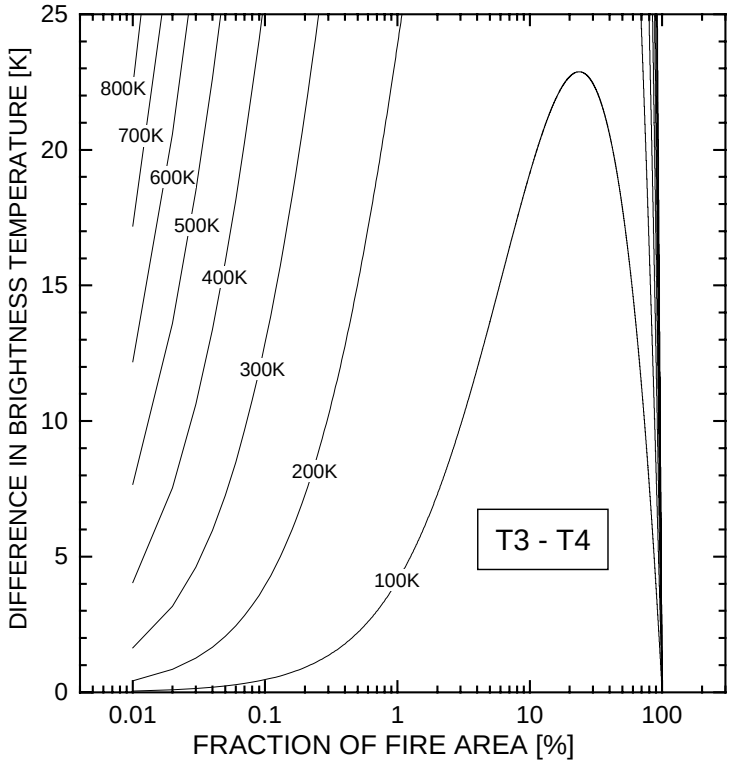

Figure 5 Difference between channel 3 and 4 TOA brightness temperatures as a function of the fraction of a fire whose temperature exceeds background temperature by an amount ranging from 100K to 800K.

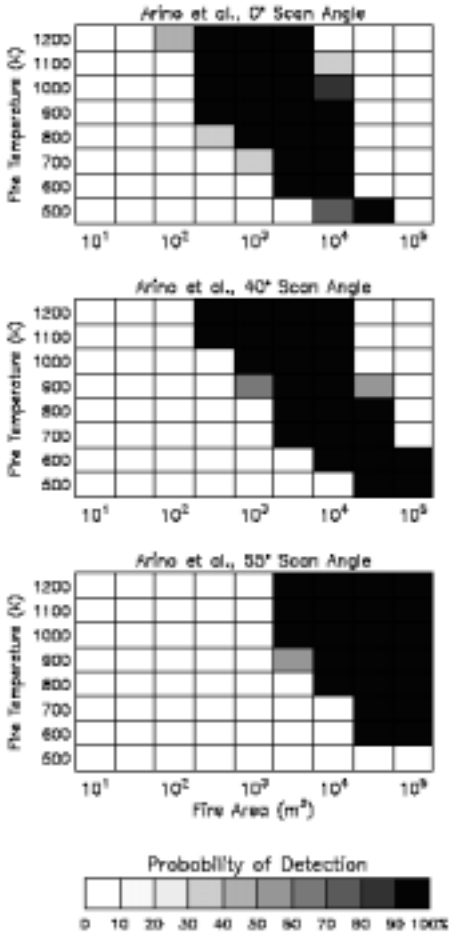

Figure 6. Fire detection envelop at scan angles of 0^o(a), 40^o(b) and 55^o(c) using the ESA algorithm (Arino et al. 1993) for fires in the tropical rain forest biome (From Giglio et al. 1999).

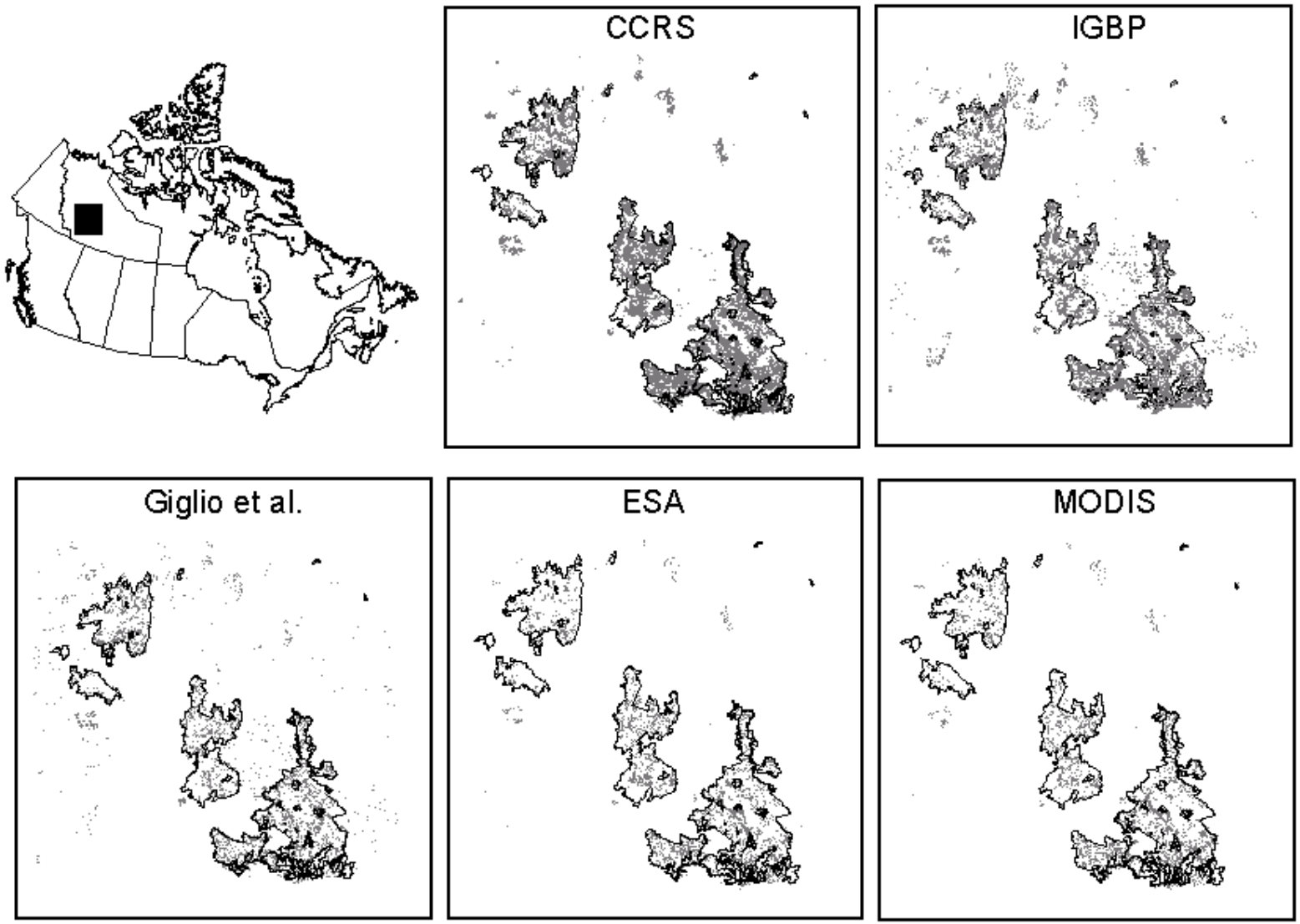

Figure 7. Comparison of fire hot spots detected by 5 algorithms against fire polygons obtained by Canadian forest agencies.

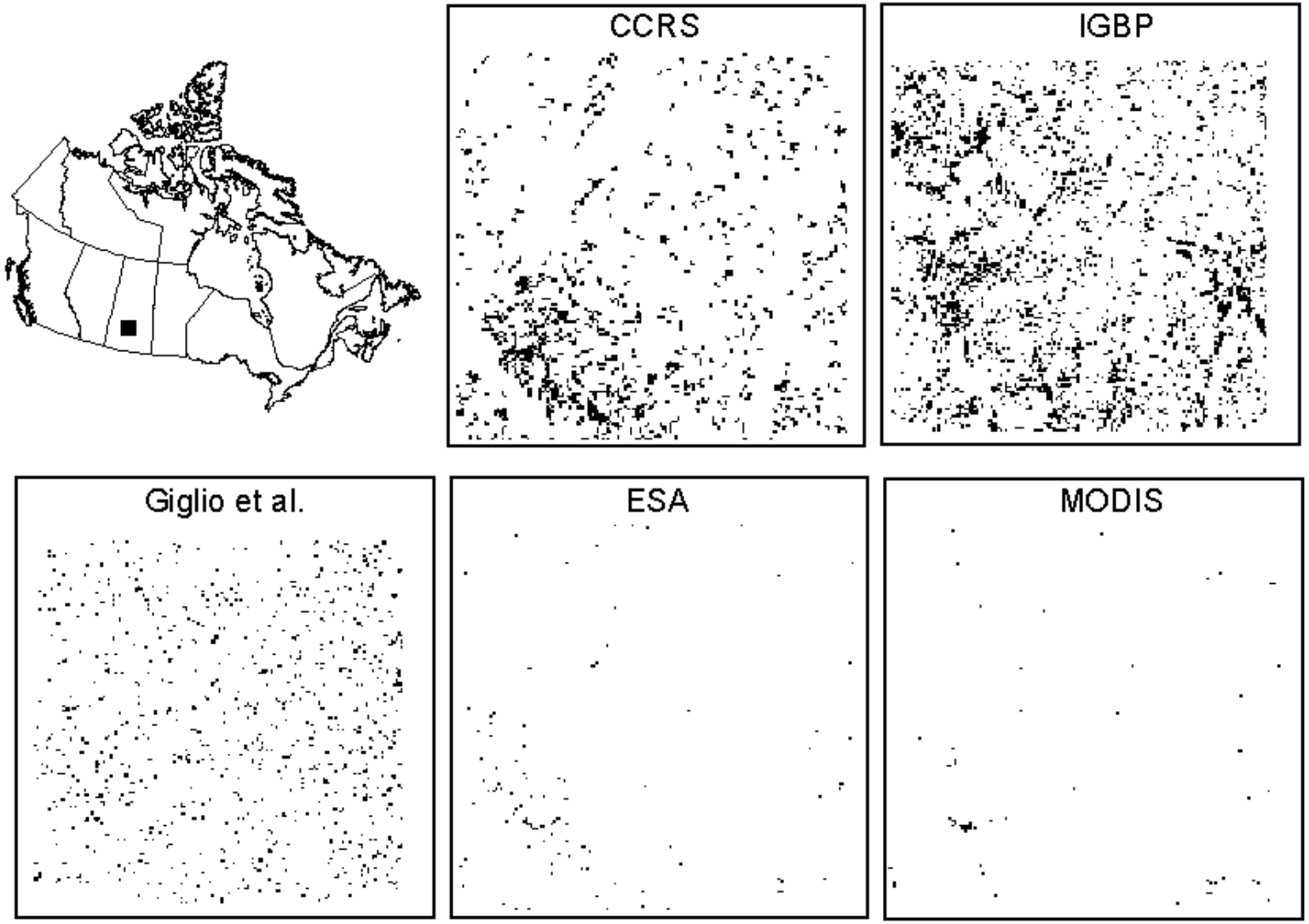

Figure 8. Comparison of fire detection results by the five algorithms over the Canadian prairies.

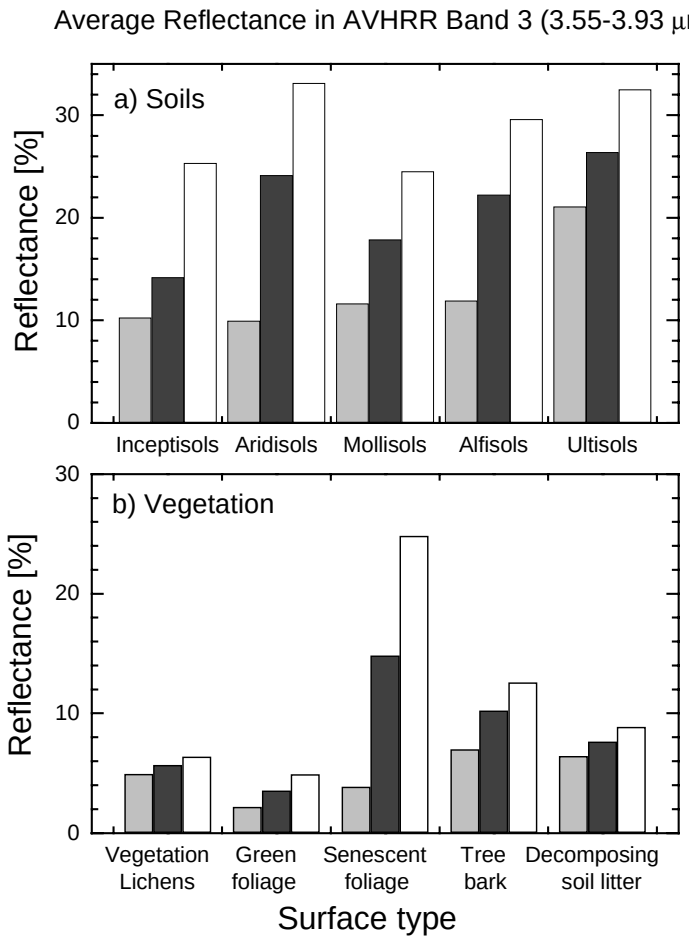

Figure 9. Mean, minimum and maximum values of the reflectivity in AVHRR channel 3 observed for many samples of soils (top) and vegetation (bottom) (reproduced from Salisbury and D'Aria, 1994).